



HAL
open science

Effect of aerated transients on stress corrosion cracking of 316L SS in high temperature water

Thalita de Paula, Marc Maisonneuve, Catherine Guerre, Cécilie Duhamel, Jérôme Crepin, Ian de Curières

► **To cite this version:**

Thalita de Paula, Marc Maisonneuve, Catherine Guerre, Cécilie Duhamel, Jérôme Crepin, et al.. Effect of aerated transients on stress corrosion cracking of 316L SS in high temperature water. 21st. International Conference on Environmental Degradation of Materials in Nuclear Power Systems - Water Reactors, Aug 2023, St-John's Newfoundland, Canada. paper 89. cea-04607775

HAL Id: cea-04607775

<https://cea.hal.science/cea-04607775v1>

Submitted on 20 Sep 2024

HAL is a multi-disciplinary open access archive for the deposit and dissemination of scientific research documents, whether they are published or not. The documents may come from teaching and research institutions in France or abroad, or from public or private research centers.

L'archive ouverte pluridisciplinaire **HAL**, est destinée au dépôt et à la diffusion de documents scientifiques de niveau recherche, publiés ou non, émanant des établissements d'enseignement et de recherche français ou étrangers, des laboratoires publics ou privés.

Copyright

Effect of aerated transients on stress corrosion cracking of 316L SS in high temperature water

T. De Paula^{1,2}, M. Maisonneuve^{1,2}, C. Guerre¹, C. Duhamel², J. Crépin² and I. De Curières³

¹ Université Paris-Saclay, CEA, Service de recherche en Corrosion et Comportement des Matériaux, 91191 Gif Sur Yvette, France

² MINES ParisTech, PSL University, Centre des matériaux, CNRS UMR 7633, BP 87 91003 Evry, France

³ IRSN, Pôle sûreté nucléaire, 31 Avenue de la division Leclerc, BP 17, 92262 Fontenay-aux-Roses cedex, France

catherine.guerre@cea.fr, cecilie.duhamel@minesparis.psl.eu, jerome.crepin@minesparis.psl.eu, iandecurieres@irsn.fr

Abstract

The effect of oxygen and oxygen transients (hydrogenated-oxygenated cycling conditions) on the stress corrosion cracking behavior of a 316L austenitic stainless steel exposed to simulated PWR primary water was studied. SCC (Stress Corrosion Cracking) tests were performed using SSRT (Slow Strain Rate Tests). Various hydrogenated-oxygenated cycling conditions (duration, frequency, starting and ending conditions) were tested and compared to tests in purely hydrogenated (DH) or oxygenated (DO) high temperature water. Quantification of the cracking network (SCC initiation sites, density, crack length and depth) was performed after SCC tests. For the same mechanical conditions, the cracking networks depend on the environment (hydrogenated, oxygenated or transients conditions). Therefore, it raises the question of the effect of the loading conditions and of the environment (DH, DO or transients) on grain boundary oxidation, which is considered as a precursor to SCC. A cracking scenario based on the relationship between grain boundary oxidation and SCC will also be presented.

1. Introduction

Austenitic stainless steels (SS), such as 304L and 316L alloys, are largely used for structural components in nuclear power plants due to their good corrosion resistance, especially under high temperatures and aqueous environments. However, operational experience on the primary circuit of pressurized water reactors (PWR) has shown an increasing number of cases of stress corrosion cracking (SCC) on austenitic stainless steels components after long-term exposure [1,2].

Austenitic stainless steels in PWR plants are often cold-worked, either purposefully to increase material strength or as an unavoidable result of manufacturing, such as bending, surface preparation, welding, and installation [3]. Previous studies have shown that cold-work as well as off-normal conditions significantly accelerates the SCC of austenitic stainless steels in simulated primary water [1, 3–8]. In normal PWR operating conditions, the primary water is deaerated and the dissolved hydrogen (DH) concentration is usually kept in the range of 25 to 35 cc.kg⁻¹(H₂O) (2.2 to 3.1 ppm) to decrease the electrochemical corrosion potential and minimize corrosion and SCC. However, during some PWR operating phases, dissolved oxygen (DO) in the primary water and oxygen transients are likely to occur [2,9–14].

Thus far, very little research has been done to understand the effects of DO and oxygen transients on the oxidation and SCC behavior of a cold-worked austenitic stainless steel in PWR primary water [11–19].

Maisonneuve et al. and De Paula et al. [11, 16-17] showed that the oxidation and SCC susceptibility of a cold-worked 316L SS in a PWR primary environment are very different in the presence of DO. In hydrogenated deaerated primary water, the inner oxide layer is Cr-rich with oxide penetrations at the grain boundaries. On the contrary, in oxygenated water and for hydrogenated-oxygenated water cycles, the inner oxide layer contains no Cr, except a very thin Cr-rich film at the metal-oxide interface and no intergranular (IG) oxidation is observed. Surprisingly, lower crack density and smaller cracks are observed under oxygenated conditions after slow strain rate tensile tests (SSRT) whereas the susceptibility to SCC initiation seems to depend on the time spent under hydrogenated conditions whatever the type of transients [11, 16].

In this context, this work aims to confirm and complete the results described previously by Maisonneuve et al. and De Paula et al. [11, 16] on the effect of DO and oxygen transients on SCC behavior of a cold-worked 316L SS in PWR primary water. For this purpose, additional SCC and oxidation tests are performed with different test procedures for the different environments (DH, DO and transients). The effect of cold work and of stress on GB oxidation is also characterized. For all environments, oxidation and SCC specimen are characterized using scanning electron microscopy (SEM), with a special emphasis on the IG oxidation and cracking network (SCC initiation sites, density, crack length, and depth).

2. Material and experimental procedure

2.1 Material

One-directionally cold-rolled 316L SS was used in this study. The material chemical composition is reported in Table 1. Before exposure to PWR primary water, the material was solution-annealed at 1050°C for 1 hour under an argon overpressure, followed by oil quenching. Optical microscopy and Electron Back Scattered Diffraction (EBSD) examinations confirmed that the resulting microstructure mostly consists of equiaxed austenite grains with an average grain size of $39 \pm 5 \mu\text{m}$, with 3% (surface fraction) of δ -ferrite bands parallel to the rolling direction (RD). No crystalline texture was evidenced.

Table 1 Chemical composition (in wt.%) of the studied 316L stainless steel.

C	Ni	Cr	Mn	Mo	Si	P	S	N	Fe
0.016	10	16.54	1.86	2.03	0.62	0.026	0.001	0.022	Bal.

2.2 Experimental procedure

2.2.1 Sample preparation

Oxidation tests are performed on non cold-worked rectangular specimens, on pre-strained specimen and on specimen loaded in the elastic region (figure 1). SCC tests are performed on flat tensile specimens (figure 1). All samples were mechanically ground with waterproof abrasive SiC paper up to 4000 grit, followed by 3, 1, and 0.25 μm diamond pastes successively and 40 nm colloidal silica suspension polishing. After that, all samples were immersed into distilled water and alcohol to remove surface contaminants by ultrasonic cleaning.

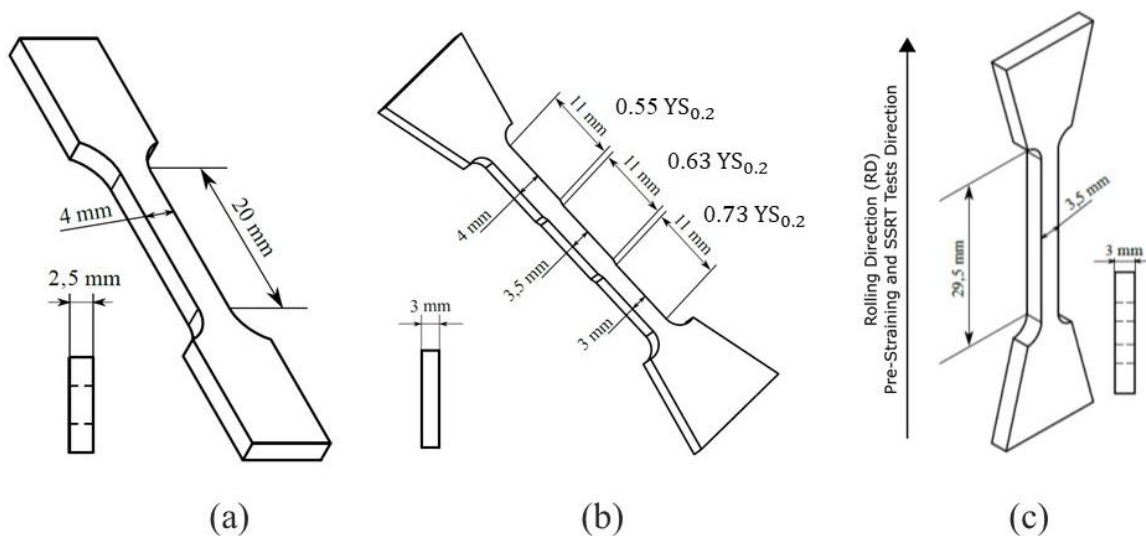


Figure 1 Geometry of (a) pre-strained specimen (b) specimen tested under constant load and SSRT specimen.

2.2.2 Oxidation tests

For the pre-strained specimen, the prestraining is performed by a tensile test in air at room temperature, at a strain rate of $5 \times 10^{-4} \text{ s}^{-1}$ up to 11% or 20% strain. For the oxidation tests performed under constant load (in the elastic region), non pre-strained flat tensile specimen with various sections (Figure 1) are used. Three sections are machined in one specimen leading to an applied stress ratio over yield stress ranging from 0.55 to 0.73 considering a yield stress of 146 MPa at 340°C (the oxidation and SCC test temperature).

After exposure, the surface oxide layer thickness and the intergranular oxide penetrations networks are characterized by SEM observations in cross-section over a length of 5 mm, which corresponds to a population of about 130 grains. In this paper, only the results on IG oxidation will be presented, the surface oxide layer characterizations are presented elsewhere [16–17].

2.2.3 SCC tests

After surface preparation, SSRT samples were tensile pre-strained in air and at room temperature, at a strain rate of $5 \times 10^{-4} \text{ s}^{-1}$ up to 11% strain, following [11,16] experimental protocol. The samples are pre-strained in order to increase SCC susceptibility [18–20]. Both pre-straining and SSRT tests were performed in the same direction (figure 1). Following Maisonneuve et al. [11] experimental protocol, SCC tests were conducted in two steps. First, the samples are oxidized under oxygenated or hydrogenated conditions for 150 hours without mechanical loading (pre-oxidation). Then, SSRT test is performed by applying a strain rate of $1.7 \pm 1.0 \times 10^{-5} \text{ s}^{-1}$ until the load reaches 60% of the yield stress, thereafter the strain rate is adjusted to $1.7 \pm 0.3 \times 10^{-8} \text{ s}^{-1}$. The test is stopped after 905 hours of loading which correspond to a final plastic strain of around 5 %.

After exposure, the SCC cracking network is characterized by SEM observations at the surface and in cross-section. Surface quantification is conducted over an area of 1 mm^2 , which corresponds to a population of over 800 grains. This area is then supposed to be statistically representative of the behavior of the whole SSRT sample. Quantifications in cross-section are performed over a length of 5 mm, which

corresponds to a population of about 130 grains. In agreement with the protocol adopted in a previous work [11], only defects deeper than 2 μm are considered as SSC cracks.

2.2.4 Water chemistry

All SSRT and oxidation tests were conducted in a 3-liter autoclave made of nickel-based alloy coupled with a recirculation water loop (flow rate: 5L/h) at 345°C and 170 bar. The simulated PWR primary water was prepared by mixing distilled water with ≈ 2 ppm of lithium and ≈ 1000 ppm of bore. The pH of the primary water is alkaline, around 7.2 at 300°C, while neutral pH is 5.7 at this temperature. The tests were performed in fully-hydrogenated or fully-oxygenated conditions or in transients conditions at 340°C. The hydrogenated conditions are defined by a dissolved hydrogen concentration of ≈ 2.6 ppm whereas the oxygenated conditions correspond to a dissolved oxygen concentration of ≈ 11 ppm. The tests are summarized in table 2.

Depending on the test, the 150 h pre-oxidation is performed in hydrogenated or oxygenated conditions, then the SSRT (start of the loading) consist of one single step with no transient, or of one single change from oxygenated water to hydrogenated water or of several changes from hydrogenated water to oxygenated water and vice versa. Thanks to these different procedures, different cumulated times in hydrogenated or oxygenated conditions during SSRT tests ranging from 0 to 905 h can be compared.

Table 2 Summary of the tested conditions.

Test	Preoxidation (150 h)	Cumulated exposure time during SSRT (h)		Number of cycles	Cycle duration (h)
		DO	DH		
150H-905H	H₂	0	905	Fully hydrogenated	
150(O)-905H	O₂	0	906	Only one change from DO to DH	
150H-80H20(O)	H₂	146	716		
150(O)-20(O)80H	O₂	239	679		
150(O)-40(O)60H	O₂	393	486		
150H-20H80(O)	H₂	681	240	5	168
150(O)-905(O)	O₂	903	0	Fully oxygenated	

3. Results

3.1 Stress corrosion cracking

Except by water chemistry, all SSRT tests presented here are performed exactly the same way, i.e. with strictly the same mechanical loading and total duration (≈ 1055 h). SEM observations of the surface of the SSRT samples reveal the presence of several cracks for all the tested specimens. Regardless of the test conditions, cracks are intergranular and oriented perpendicularly to the pre-strain and SSRT direction (Figure 2). Several transgranular (TG) crack-like defects are also observed (Figure 2). However, as these defects are very small and their mean depth is shorter than the inner-oxide layer thickness, they are not considered as SCC cracks and they were not quantified. Cracking networks were characterized on surface and on cross-sections : the results are presented on figures 3 and 4. In all cases, the crack density increases over the time spent in hydrogenated conditions, as for the crack length (on surface) and crack depth on cross-sections. Therefore, it can be concluded that for the same mechanical conditions, the susceptibility to stress corrosion cracking strongly depends on the effect of the dissolved gas during the different stages of the SSRT tests. Indeed, the SSRT can be represented by three stages: pre-oxidation (on pre-strained specimen), elastic region during SSRT and plastic region during SSRT (Figure 5). Therefore, the oxidation during these different steps has been studied separately.

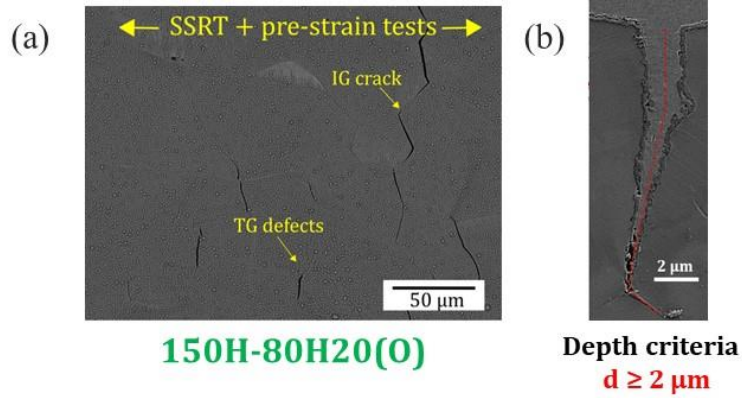


Figure 2 SSRT specimen tested with transients conditions at 340°C (a) SEM image of the surface showing TG defects and IG SCC cracks (b) SEM image of a IG crack

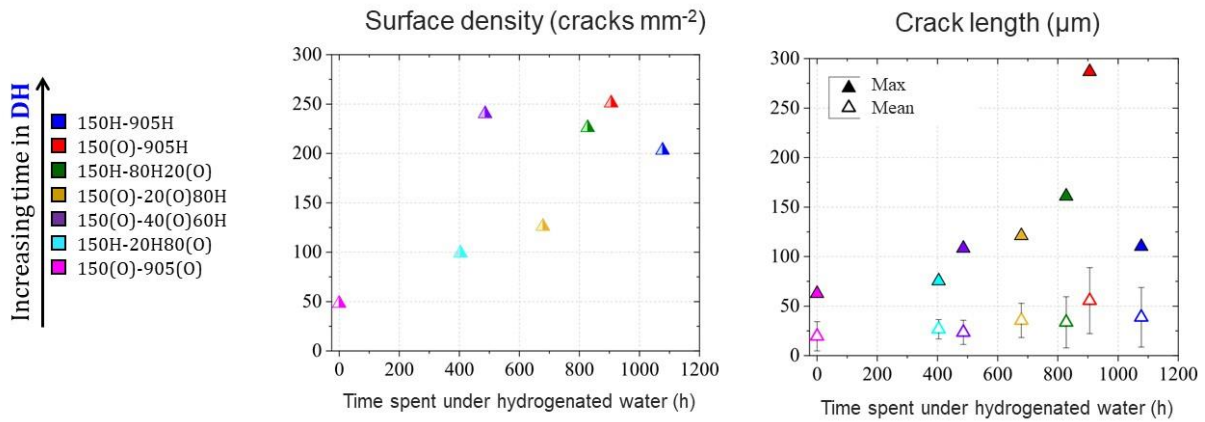


Figure 3 SCC crack surface density and length over the cumulated time spent in hydrogenated water at 340°C (SSRT tests).

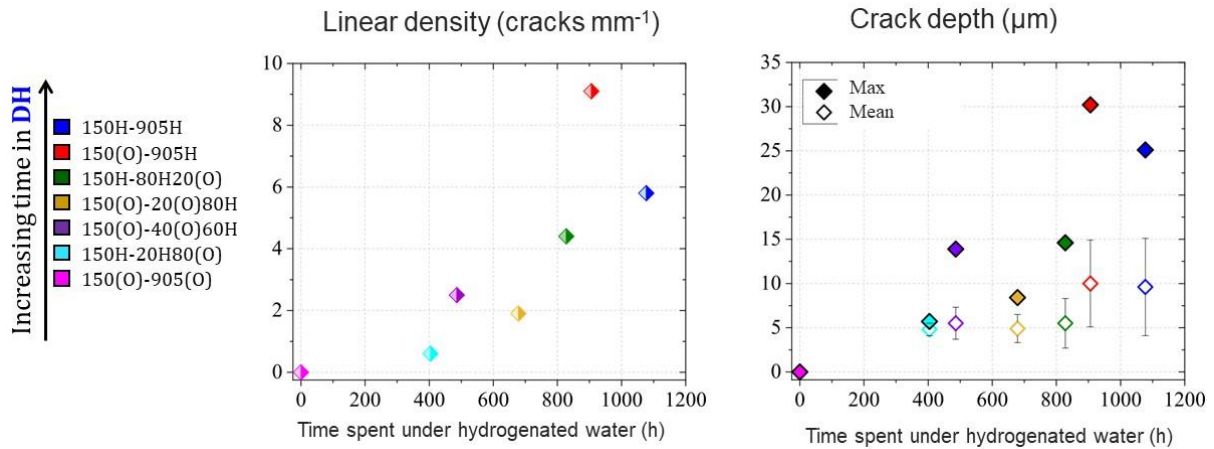


Figure 4 SCC crack (> 2 μm) linear density and depth over the cumulated time spent in hydrogenated water at 340°C.

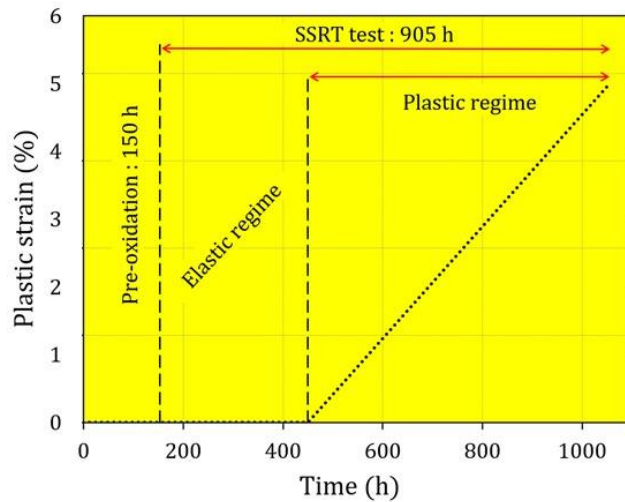


Figure 5 Schematic representation of the slow strain rate test.

3.2 Oxidation on coupons

The surface oxidation behavior on coupons (no pre-oxidation) has been studied in [11, 16–17]. The main results are that the surface oxide layer is similar for fully-oxygenated water and the tested transients conditions. The oxide formed in hydrogenated water is modified during a following exposure in oxygenated water. Then further short-term exposures (few tens of hours) in hydrogenated water don't modify anymore the oxide layer that was previously formed in oxygenated water. Another significant result is that intergranular oxide is only evidenced on coupons exposed to fully-hydrogenated water or transients conditions with the longer exposures to hydrogenated water. In fully hydrogenated water, despite a low density and strong scattering, it can be evidenced that IG oxidation increases with time (figure 6). The maximum percentage of oxidized GBs is below 20 % for oxidation times up to 5000 h, it corresponds to a maximum of half the HAGBs. It is consistent with the fact that the susceptibility to IG oxidation depends on GB properties. The same conclusion on the effect of time spent under hydrogenated conditions on GB oxidation can be drawn when including tests with transients conditions. Nevertheless,

the result should be considered with caution due to the very low density of oxidized GBs observed for shorter cumulated exposure time to hydrogenated water (Figure 7). No IG oxide penetration was observed for coupons tested under fully- oxygenated conditions. Taking into account the fact that intergranular oxide penetrations are considered as the precursors to SCC crack initiation [4, 11, 16, 21] the study will focus on it.

During pre-oxidation (first step of the SSRT test), the specimen is pre-deformed and exposed to hydrogenated or oxygenated primary water. Therefore, the effect of this predeformation on IG oxidation will be studied.

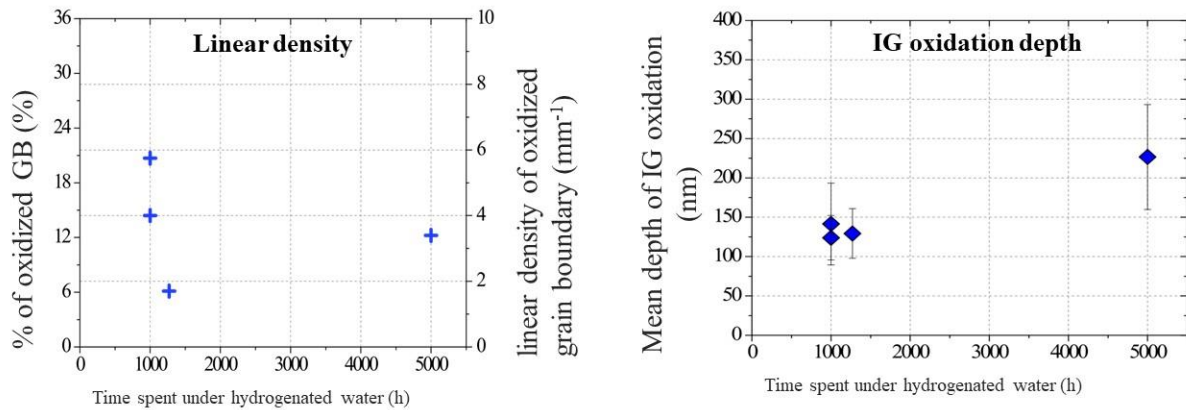


Figure 6 IG oxide penetrations density and depth over the time spent in hydrogenated water : coupons tested at 340°C in fully-hydrogenated conditions.

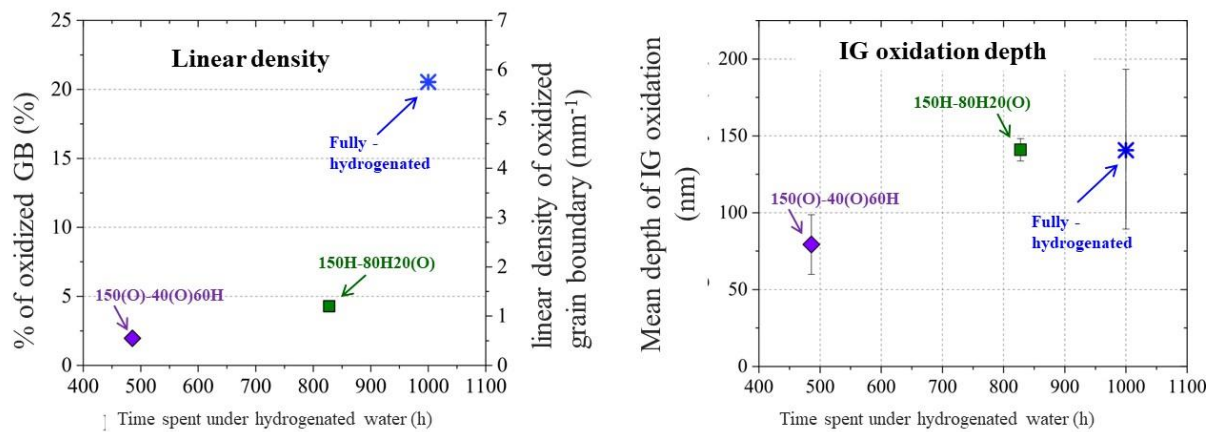


Figure 7 IG oxide penetrations density and depth over the time spent in hydrogenated water : coupons tested at 340°C with transients conditions or in fully-hydrogenated conditions.

3.3 Intergranular oxidation : effect of predeformation and stress

Before SSRT, the specimen are pre-deformed up to 11 %. In order to study the effect of predeformation on IG oxidation, specimen were pre-deformed to the same level but also to 20 %. The results of the characterization of the cross-sections (IG oxide penetrations density and depth) are presented in figure 8. Whatever the predeformation and the environment (DO, DH or transients), the predeformation does

not significantly increase the susceptibility to IG oxidation. Furthermore, there is still no IG oxidation for tests performed in oxygenated water.

The same characterizations have been made on non-deformed specimens tested under constant load in fully hydrogenated or fully oxygenated water during 1000 h, which simulates the second step of the SSRT test (elastic region at the beginning of the test), apart from the absence of predeformation. Transients conditions have not been tested. In this case, the applied stress significantly increases the density and depth of IG oxide penetrations in hydrogenated water (Figure 9). In fully-oxygenated water, it induces IG oxidation which was not observed for all the other conditions tested (Figure 9).

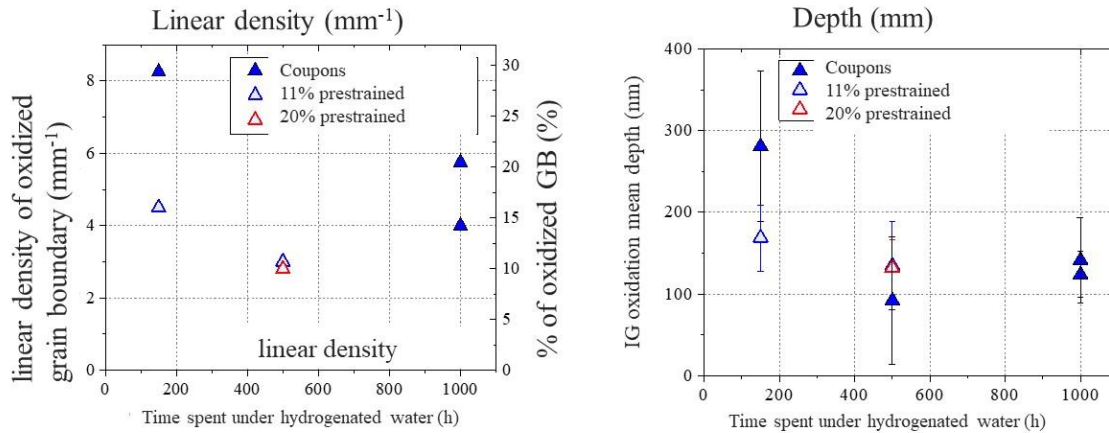


Figure 8 IG oxide penetrations density and depth over the cumulated time spent in hydrogenated water : comparison between coupons and pre-streined specimen tested at 320°C (150 h tests) and 340°C.

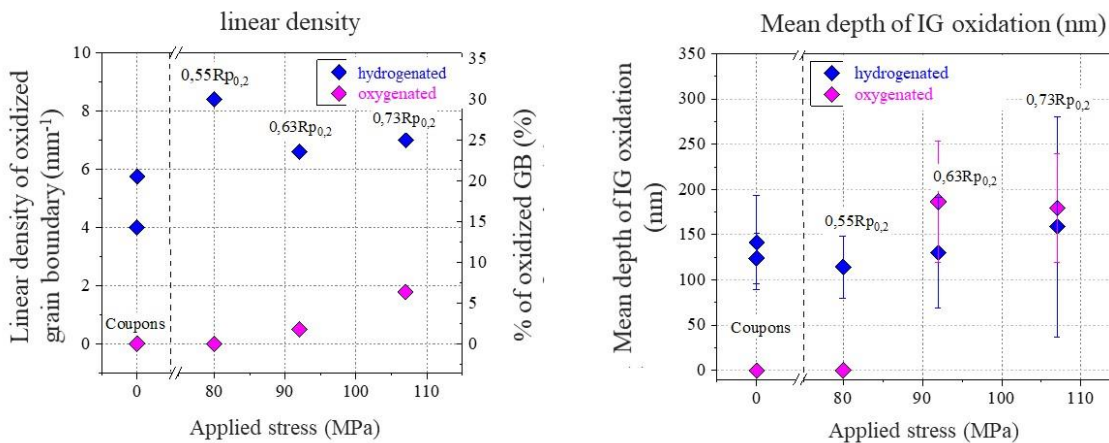


Figure 9 IG oxide penetrations density and depth over the applied stress in hydrogenated and oxygenated water : specimens tested 1000 h at 340°C.

3.4 Intergranular oxidation after SSRT

The IG oxidation is also characterized on SSRT specimens (Figure 10). The density and depth are greater than for coupons or pre-strained specimens but remains below 5 μm . The reason is that, after SSRT tests, other intergranular features are observed (Figure 11):

- Some GBs are still not oxidized.
- Others are oxidized and not cracked.
- The third types are oxidized and cracked (with a depth below 2 μm) GBs: they are considered as initiating cracks.
- Finally, some GBs are oxidized and their crack depth is above 2 μm : they are considered in this study as SCC cracks.

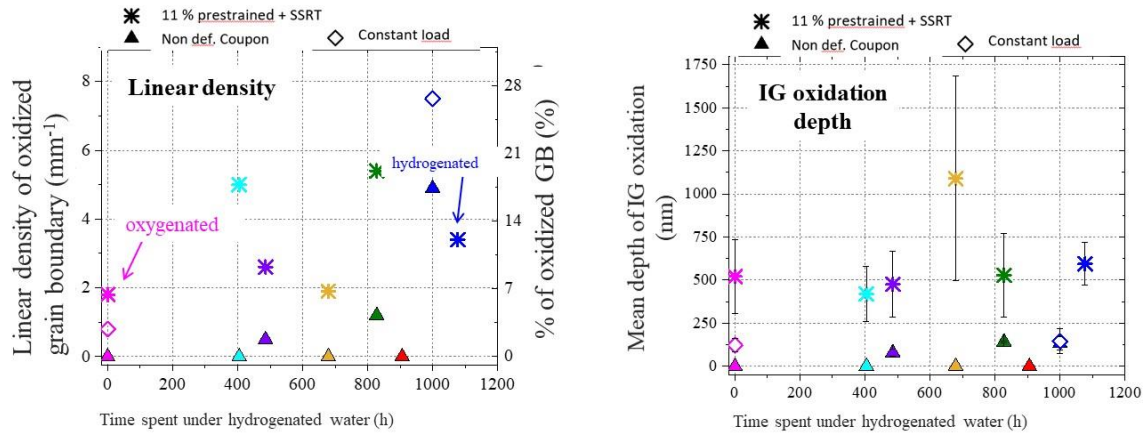


Figure 10 IG oxide penetrations density and depth over the cumulated time spent in hydrogenated water : comparison between coupons, pre-deformed specimens, specimens tested under constant load and SSRT specimens at 340°C. The total oxidation time is 1000h in all cases.

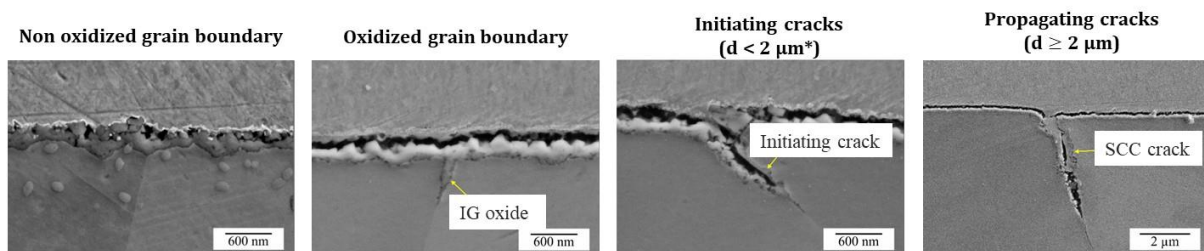


Figure 11 Different GB types observed for SSRT tests (cross-section characterizations by SEM).

4. Discussion

Considering the results concerning the effect of predeformation, stress and water chemistry on IG oxidation, a cracking scenario can be suggested.

4.1 Assumptions

The oxidation tests results lead to the following conclusions that will be considered as assumptions for the cracking scenario :

- The 150 h pre-oxidation step can be dismissed (short exposure time leading to a low number of oxidized GBs with small depth in hydrogenated water; no IG oxidation in oxygenated water).
- The order and duration of transients can be neglected.
- Applied stress increases the IG oxidation, in particular in the plastic domain.
- Both IG oxidation and SCC crack initiation increase over the time spent in hydrogenated water. It is consistent with an assumed mechanism which implies the failure of an oxidized GB when a critical oxidation depth coupled with normal stress is attained [21]. On the same material, a correlation between the most stressed and the failed GB has been established [22] even if it was shown that is not a sufficient criterion to account for SCC initiation. In particular, the intergranular oxidation depth has to be considered (as it is for the coupled criterion).
- Discontinuous crack advance (propagation) by continuous oxidation in hydrogenated water of HAGBs followed by their failure when the coupled IG oxidation depth / normal stress criterion is reached.

4.2 Cracking scenario

Based on the previous assumptions, the following scenario (Figure 12) is suggested for SSRT on pre-strained specimens tested in primary water (for hydrogenated or transients conditions).

The oxidation depth increases over the time spent in hydrogenated water, i.e. over test time during SSRT test. The mean and maximum IG oxidation depths increase over time. Quantifications performed on cross sections permit to give IG oxidation depth range for GB failure. Below 400 nm, no oxidized GB fails. The first GB failure occurs for a depth in the range 400 nm – 700 nm. It is the start of the initiation stage. Then over test time, the fracture probability increases and the density of failed GB increases due to the increase of the oxidation depth and of the GB stress [22]. Then, for oxidation depth above 1,5 μm, there is a systematic fracture of the GBs. Above 2 μm, it is the crack advance stage (domain 2), that is defined by a mean crack advance of about 0.2 mm/year. In our conditions, it can be considered as the short crack regime. The propagation stage is usually observed for longer crack (above one grain size).

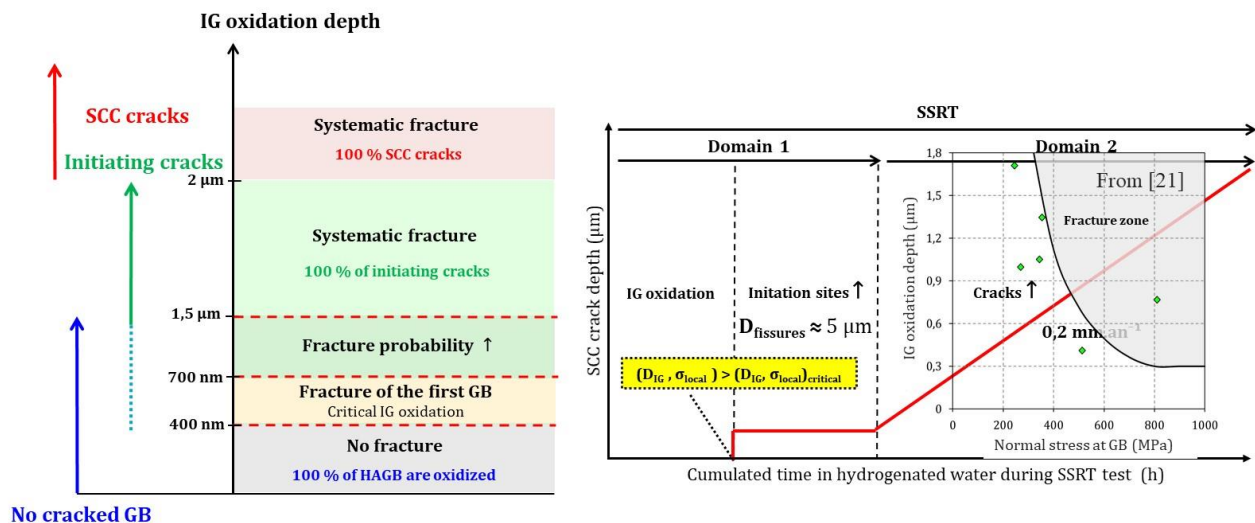


Figure 112 Cracking scenario for SSRT SCC on pre-strained 316 L in primary water (with transients conditions).

5. Conclusion

In this work, we analyze the effects of oxygen transients on SCC susceptibility and intergranular oxidation of 316L SS in PWR primary water at 340°C. SCC was evaluated by SSRT tests. After tensile testing, leading to $\approx 5\%$ plastic strain, intergranular SCC cracks were observed in all the tested conditions. However, the SCC susceptibility increases with the cumulated time spent under hydrogenated conditions.

After exposure to different transient conditions on non pre-strained, pre-strained and stressed specimens, it has been shown that IG oxidation (density and depth) increases over the time spent in hydrogenated water and is promoted by stress (elastic region). IG oxidation is also promoted by SSRT conditions that imply a continuous increase of the stress and strain at GB along test time. Furthermore, the IG oxidation depth also increases over test time. According to the coupled oxidation depth / stress criterion, it leads to an increase of failed oxidized grain boundaries, and then of the initiating cracks density along the test.

The suggested cracking scenario is based on a continuous increase of the number of GBs (HAGBs) fulfilling the failure criterion, followed by a propagation stage based on a discontinuous crack advance by continuous oxidation in hydrogenated water of HAGBs followed by their failure when the coupled IG oxidation depth / normal stress criterion is fulfilled.

For fully oxygenated conditions, no IG oxidation was observed on coupons and on pre-strained specimen (up to 20 % plastic deformation). Stress appears to be a necessary condition to induce IG oxidation. Further experiments will be performed in order to confirm this result at different stress levels and at different temperatures. More characterizations are also needed to better understand the IG oxidation mechanism and kinetics in oxygenated water under stress but also in hydrogenated water. There is still very few quantitative results in the literature and no mechanism for preferential intergranular oxidation is proposed.

For the tested conditions (SSRT), oxygenated water transients do not increase the susceptibility to SCC of stainless steels in PWR primary water. These results are not in agreement with the operating experience, which could be explained by the type of SCC tests performed in laboratory. Different SCC tests procedures have to be tested in order to better understand this apparent discrepancy.

6. References

- [1] T. Couvant, C. Varé, J.M. Frund, Y. Thébault, B. Audebert et E. Lemaire, "Susceptibility to IGSCC of cold worked austenitic stainless steels in non-polluted primary PWR environment" International Symposium Fontevraud 10 (Avignon, 2022).
- [2] G.O. Ilevbare, F. Cattant, N.K. Peat, "SCC of Stainless steels under PWR service conditions," International Symposium Fontevraud 7 (Avignon, 2010).
- [3] J. Chen, Z. Lu, Q. Xiao, X. Ru, G. Han, Z. Chen, B. Zhou, T. Shoji, "The effects of cold rolling orientation and water chemistry on stress corrosion cracking behavior of 316L stainless steel in simulated PWR water environments," *Journal of Nuclear Materials* 472 (2016): pp. 1–12.
- [4] T. Couvant, D. Haboussa, S. Meunier, G. Nicolas, E. Julan, K. Sato, F. Delabrouille, "A Simulation of IGSCC of Austenitic Stainless Steels Exposed to Primary Water," 17th International Conference on Environmental Degradation of Materials in Nuclear Power Systems – Water Reactors (Ottawa, 2015).
- [5] P. Huguenin, J. Crépin, C. Duhamel, H. Proudhon, F. Vaillant, "Initiation of Stress Corrosion Cracking in pre-strained austenitic stainless steels exposed to primary water," 16th

International Conference on Environmental Degradation of Materials in Nuclear Power Systems – Water Reactors (Asheville, 2013).

- [6] S. Lozano-Perez, T. Yamada, T. Terachi, M. Schröder, C.A. English, G.D.W. Smith, C.R.M. Grovenor, B.L. Eyre, "Multi-scale characterization of stress corrosion cracking of cold-worked stainless steels and the influence of Cr content," *Acta Materialia* 57, 18 (2009): pp. 5361–5381.
- [7] T. Shoji, K. Sakaguchi, Z. Lu, S. Hirano, Y. Hasegawa, T. Kobayashi, K. Fujimoto, Y. Nomura, "Effects of cold work and stress on oxidation and SCC behavior of stainless steels in PWR primary water environments," *International Symposium Fontevraud 7* (Avignon, 2010).
- [8] T. Terachi, T. Yamada, T. Miyamoto, K. Arioka, "SCC growth behaviors of austenitic stainless steels in simulated PWR primary water," *Journal of Nuclear Materials* 426, 1-3 (2012): pp. 59–70.
- [9] J. Chen, Q. Xiao, Z. Lu, X. Ru, H. Peng, Q. Xiong, H. Li, "Characterization of interfacial reactions and oxide films on 316L stainless steel in various simulated PWR primary water environments," *Journal of Nuclear Materials* 489 (2017): pp. 137–139.
- [10] J. Xu, S. Xia, X. Zhong, T. Shoji, "The Corrosion Behavior of Nickel-Based Alloys 182 and 52 and 316 Stainless Steel in Cyclic Hydrogenated and Oxygenated Water Chemistry in High Temperature Aqueous Environment," *17th International Conference on Environmental Degradation of Materials in Nuclear Power Systems – Water Reactors* (Ottawa, 2015).
- [11] M. Maisonneuve, C. Duhamel, C. Guerre, J. Crépin, I. de Curières, "Effect of Aerated Transients on Oxidation and SCC of Stainless Steels in PWR Primary Water. In: *19th International Conference on Environmental Degradation of Materials in Nuclear Power Systems – Water Reactors*," (Boston, 2019).
- [12] M. Herbst, R. Kilian, O. Calonne, N. Huin, "SCC of Austenitic Stainless Steels Under Off-Normal Water Chemistry and Surface Conditions - Part II : Off Normal Chemistry - Long Term Oxygen Conditions and Oxygen Transients," *18th International Conference on Environmental Degradation of Materials in Nuclear Power Systems – Water Reactors* (Portland, 2017).
- [13] N. Huin, O. Calonne, S. Berger, B. Devrient, R. Kilian, L. Fournier, A. Marion, "Stress Corrosion Cracking of stainless steels tested by dynamic loading in oxidizing and reducing PWR primary environment," *17th International Conference on Environmental Degradation of Materials in Nuclear Power Systems – Water Reactors* (Ottawa, 2015).
- [14] N. Huin, O. Calonne, M. Herbst, R. Kilian, "SCC of Austenitic Stainless Steels Under Off-Normal Water Chemistry and Surface Conditions - Part I : Surface Conditions and Baseline Tests in Nominal PWR Primary Environment," *18th International Conference on Environmental Degradation of Materials in Nuclear Power Systems – Water Reactors* (Portland, 2017).
- [15] Y-J. Huang, T. Yamaguchi, H. Murai, H. Sugino, T. Nakajima, M. Nono, K. Kawakita, A. Kimura, "SCC susceptibility of solution-annealed 316L SS in hydrogenated hot water below 288 °C," *Corrosion Science* 145 (2018): pp. 1–9.
- [16] T. De Paula, C. Duhamel, C. Guerre, J. Crépin, I. de Curières, F. Datcharry, M. Maisonneuve "Effect of dissolved oxygen on the SCC susceptibility and oxidation of cold-worked 316L SS

in PWR primary water”, 20th International Conference on Environmental Degradation of Materials in Nuclear Power System – Water Reactors (Snowmass village, 2022).

- [17] C. Duhamel, T. De Paula, M. Maisonneuve, C. Guerre, J. Crépin, I. de Curières, “TEM characterization of surface and crack oxidation of 316L SS in PWR water after hydrogenated-oxygenated cycles”, 21st International Conference on Environmental Degradation of Materials in Nuclear Power System – Water Reactors (Saint John’s, 2023).
- [18] O. Raquet, E. Herms, F. Vaillant, T Couvant, J-M. Boursier, “SCC of cold-worked austenitic stainless steels in PWR conditions,” 12th International Conference on Environmental Degradation of Materials in Nuclear Power System – Water Reactors (Salt Lake City, 2005).
- [19] M. Rousseau, E. Herms, F. Vaillant, “Characterization of SCC cracks in a cold-worked 316L austenitic stainless steel after exposure to PWR primary water conditions,” Eurocorr (Estoril, 2013)
- [20] T. Couvant, L. Legras, F. Vaillant, J-M. Boursier, Y. Rouillon, “Effect of strain-hardening on Stress Corrosion Cracking of AISI 304L stainless steel in PWR primary environment at 360°C” 12th International Conference on Environmental Degradation of Materials in Nuclear Power System – Water Reactors (Salt Lake City, 2005).
- [21] Q. Huang, “Analyse expérimentale et numérique de l’amorçage de fissures de corrosion sous contrainte dans les aciers inoxydables pré-écrouis” PSL University and Paris-13 University PhD thesis, 2019.
- [22] Q. Huang, Y. Charles, C. Duhamel, M. Gaspérini, J. Crépin, “Influence of the combination of microstructure and mechanical fields on stress corrosion cracking initiation of cold-worked austenitic stainless steels” 19th International Conference on Environmental Degradation of Materials in Nuclear Power System – Water Reactors (Boston, 2019).